Nuclear Inst. and Methods in Physics Research, A 879 (2018) 147–152

Contents lists available at ScienceDirect

Nuclear Inst. and Methods in Physics Research, A

journal homepage: www.elsevier.com/locate/nima

Design of a portable dose rate detector based on a double Geiger–Mueller counter

Peng Wang [a], Xiao-Bin Tang [a,b,*], Pin Gong [a,b], Xi Huang [a], Liang-Sheng Wen [a], Zhen-Yang Han [a], Jian-Ping He [a]

[a] Department of Nuclear Science and Engineering, Nanjing University of Aeronautics and Astronautics, Nanjing 210016, China
[b] Jiangsu Key Laboratory of Nuclear Energy Equipment Materials Engineering, Nanjing University of Aeronautics and Astronautics, Nanjing] 210016, China

ARTICLE INFO

Keywords:
Portable equipment
Dose rate detector
Geiger–Mueller counter
Energy compensation

ABSTRACT

A portable dose rate detector was designed to monitor radioactive pollution and radioactive environments. The portable dose detector can measure background radiation levels (0.1 μSv/h) to nuclear accident radiation levels (>10 Sv/h). Both automatic switch technology of a double Geiger–Mueller counter and time-to-count technology were adopted to broaden the measurement range of the instrument. Global positioning systems and the 3G telecommunication protocol were installed to prevent radiation damage to the human body. In addition, the Monte Carlo N-Particle code was used to design the thin layer of metal for energy compensation, which was used to flatten energy response The portable dose rate detector has been calibrated by the standard radiation field method, and it can be used alone or in combination with additional radiation detectors.

1. Introduction

Nuclear safety has become a growing concern because of the widespread application of nuclear technology in daily life. Nuclear facilities or radioactive nuclides can release penetrating radiation into the surrounding environment; these rays can harm to the human body. However, ionizing radiation cannot be perceived by the physical senses. The use of radiation detectors is one of the most effective ways to protect against exposure to radiation. Gamma radiation is an important part of external exposure because of its strong penetrability [1]. Therefore, accurate measurement of the gamma dose rate is very important.

In recent years, various gamma detectors have been widely used for dose rate measurement, including gas detectors, scintillation and semiconductor detectors [2–4]. Among gas detectors, the Geiger–Mueller (GM) counter is commonly used to monitor the gamma dose rate [5]. The GM counter is one of the oldest existed radiation detector types; this affordable, simple, and flexible detector has numerous advantages [6,7]. The long "dead time" of the GM counter is its biggest weakness because the measurement range of the dose rate is limited by it [8]. The traditional GM counters (composed of single GM counter) have a narrow range of dose rate responses, and the effective measurement range is approximate three orders of magnitude. Normally, personnel need to carry dose rate detectors close to the target. This methodology is extremely dangerous and inconvenient. Thus, traditional detectors cannot complete necessary missions, such as unattended operation and online measurement in real time. In order to address the above-mentioned problems, an innovative dose rate detector based on the double GM counter was developed. The global positioning system (GPS) and third-generation telecommunication (3G) functionality were adopted to enhance the function of the dose rate detector.

2. Experimental

2.1. Instrument design

The innovative dose rate detector was composed of three parts: GM counter, radio frequency (RF) module, and electronic system. The electronic system (Fig. 1) included the GPS, 3G, power management, and microprogrammed control unit (MCU). The time-to-count technology [9] was used for calculating the dose rate. Thus, the MCU is an important part of the electronic system. The MCU determines the measurement range of the detector. NXP LPC 1549 [10] based on ARM Cortex-M3 [11] was adopted, with a frequency of 72 MHz. The printed circuit board (PCB) of the electronic system was designed by Cadence 16.3 [12].

* Corresponding author at: Department of Nuclear Science and Engineering, Nanjing University of Aeronautics and Astronautics, Nanjing 210016, China.
E-mail address: tangxiaobin@nuaa.edu.cn (X. Tang).

http://dx.doi.org/10.1016/j.nima.2017.07.061
Received 15 September 2016; Received in revised form 17 May 2017; Accepted 29 July 2017
Available online 9 August 2017
0168-9002/

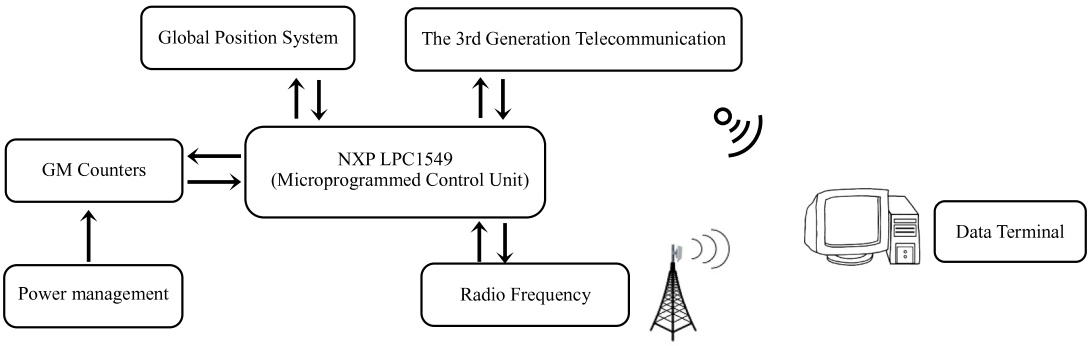

Fig. 1. Composition block diagram of the innovative dose rate detector.

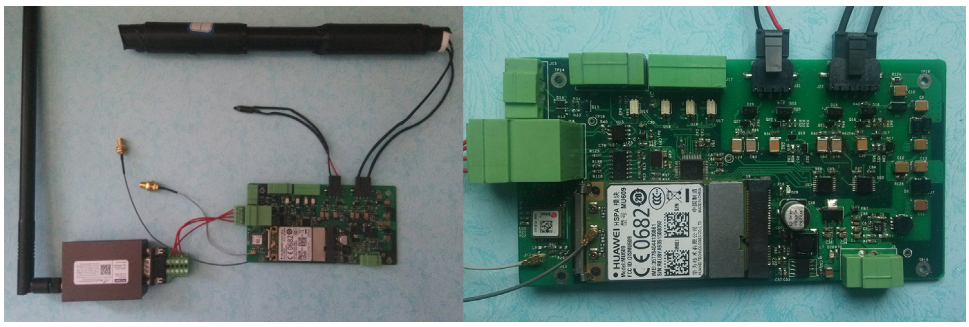

Fig. 2. Photographs of the actual dose rate detector.

The GPS and dose rate data were collected, packaged, and wirelessly transmitted to the data terminal. The detector had two wireless transmission modes. The first transmission mode is the 3G network, and the other is the RF transmission. If the monitoring sites were not covered by the 3G network, the data will be transmitted by RF. The double GM counters are composed of a large-volume GM counter and a small-volume GM counter (see Section 2.2). The large-volume GM counter was used to measure the radiation environment of the low dose rate. The small-volume GM counter was used to measure the radiation environment of the high dose rate. The RF module communicated with the electronic system via the RS-232 interface. The frequency of the radio is 900 MHz, and the radio sensitivity is −108 dBm. The highly-sensitive radio allows for data transfer up to 10 km. The weight of the detector is less than 50 g and the size is about 30 cm × 7 cm × 5 cm. The power (the data is transmitting) is 1 W, therefore two lithium batteries can make the system work correctly for 24 h. The input voltage of the system is wide (4–6 V). The detective limit of the dose rate detector increases to more than 10 Sv/h, and the detector can work well under serious nuclear accidents. Unmanned aerial vehicles and remote-controlled robots can install the innovative dose rate detector to perform the appropriate task. The dose rate detector can also be as the stationary emergency system of nuclear facilities. The sensor module is shown in Fig. 2.

2.2. Calculation of energy compensation

The photon radiation interacts with the cathode of GM counters (the wall) by Compton scattering, as well as photoelectric and electron pair effects. Electrons ejected from the wall into the gas volume create initial ionization. Electron avalanche amplification is produced by ionization of the fill gas [13]. The cathode of GM counters therefore has a very important role in the process of gamma photon detection [14–17]. The cathode of GM counters is made of metal. Compared to tissue, the metal has an over response below about 300 keV. Due to strong photoelectric interaction, the GM counter's energy response to gamma is not flat. A thin-metal wrap is used to improve the problem of the energy response [18]. The metal type, layer thickness, and covered area need to be designed [19]. The main detection components of the dose rate detector are the GM tubes. Therefore, the energy compensation needs to be designed in relation to the specific sensor.

Four metals were chosen as candidates for the energy compensation filler: tin (Sn), aluminum (Al), copper (Cu), and lead (Pb). The Monte Carlo N-Particle (MCNP) code was used to design the metal type, layer thickness, and covered area. The models of the GM counters are LND 78017 and LND 71629. The sizes of the geometric model are shown in Fig. 3. However, the sensitive volume of GM counters, which is one part of the GM counter, is the most important since this defines the length of cathode that contributes, and the filling gas of sensitive volume is a mixture of neon and bromine. The electron avalanche amplification is only produced in the sensitive volume of GM counters. The effective length of the large-volume GM counter is 241.6 mm, and the effective length of the small-volume GM counter is 6.4 mm (Fig. 3).

Both large-volume and small-volume GM counters were simulated since both had to be operated together, over their respective range to obtained accurate results. The calculation results of 24 different gamma energies were used to determine the material for energy compensation and the layer thickness. Each material corresponded to four thicknesses. The double GM counters were made of stainless steel. The sizes of the GM counter are shown in Fig. 3 and based on the introduction of products. Isotropic incidence was modeled because the application is for environmental source distribution. Results will be presented in Section 3.

2.3. Instrument calibration

Time-to-count technology and double GM counters were used to extend the measurement range in this device. The traditional measurement method uses the count rate to represent the radiation dose rate. However, the basic principle of time-to-count technology is the use of interval time instead of the count rate. The working process of the instrument is that the GM counter voltage is dropped to half its original value at the beginning of the electron avalanche; is kept low

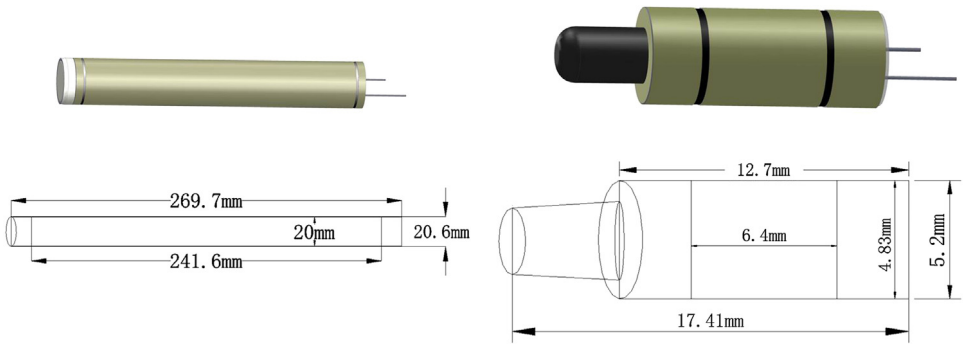

Fig. 3. Geometric models and geometric parameters of GM counters.

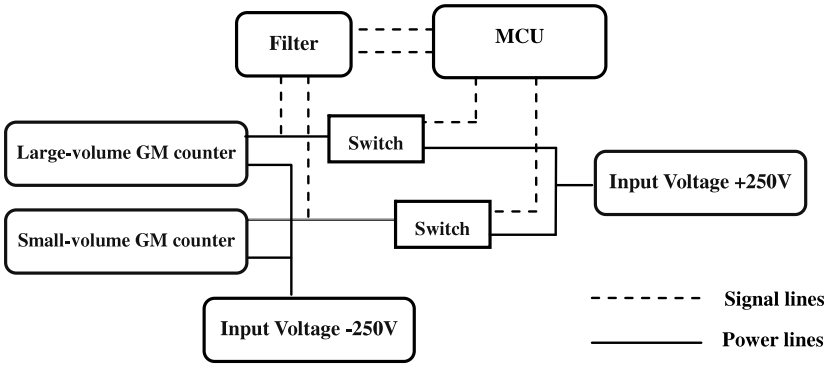

Fig. 4. Principle diagram of time-to-count technology.

Fig. 5. Calibration equipment of dose rate meter.

for a moment and then restored to its original state to complete the process. The time interval between two adjacent processes should be measured to reflect gamma ray intensity. The principle diagram of time-to-count technology is shown in Fig. 4. The operating voltage of the two GM counters was 500 V; the positive 250 V voltage and the negative 250 V voltage were produced by a DC–DC converter. The switch is applied to control the opening or closure of the high-voltage circuit. The pulse signals were denoised by a filter and transmitted to the MCU to terminate the timing signal.

The GM counter is a relative measuring instrument, which requires calibration before use. However, given the limited conditions, different kinds of radioactive sources were applied in the calibration experiments. Standard radiation fields were produced by changing the distance between instruments and sources, which were Cs-137 and Co-60. The radioactivity level of Cs-137 is relatively low, and the range of dose rate is from 5 to 200 μSv/h. The radioactivity level of Co-60 is relatively high, and the dose rate range is from 1 to 2.5 Sv/h. The National Institute of Metrology and the Measurement of Jiangsu Province Academy of Sciences provided the standard radiation fields (Fig. 5).

2.4. Outdoor experiments

The instrument has three more functions than the traditional GM counters, namely, the 3G, RF, and GPS. To test communication and application effect of this dosimeter, outdoor experiments were done in an open area. The data terminal was more than 500 m from the test area to test the RF transmission and GPS performance. In the outdoor experiments, we placed two sources in a cleared field. This field is a square with sides of approximately 10 m. The sources were placed on the ground, and the detection data were transferred to the data terminal, which is approximately 500 m from the monitoring stations. Both sources are I-131 as shown in Fig. 6.

In an indoor experiment, the detector was placed near the source, and the data terminal was moved to another room upstairs. We continuously measured this source for the next 11 h. The dose rate information was transferred to the data terminal every 1 s. The whole experiment did not need to be manned, and the dose rate information was automatically written to the database of the computer terminal. The indoor experiment

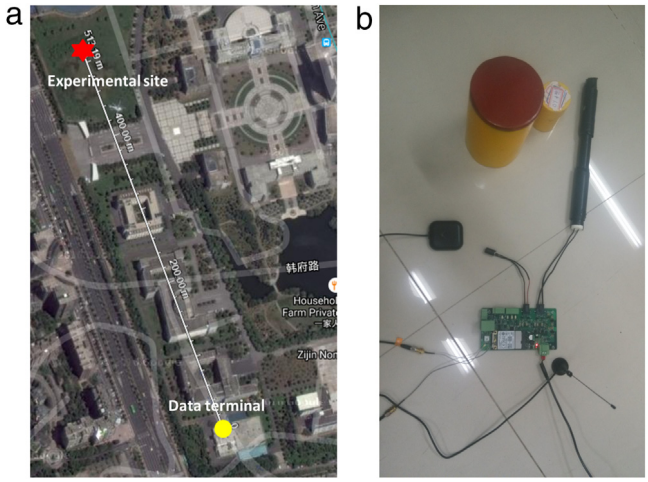

Fig. 6. Photographs of actual environment experiments. (a) The position of outdoor experiment on the map; (b) relative position between the instrument and source in indoor experiment

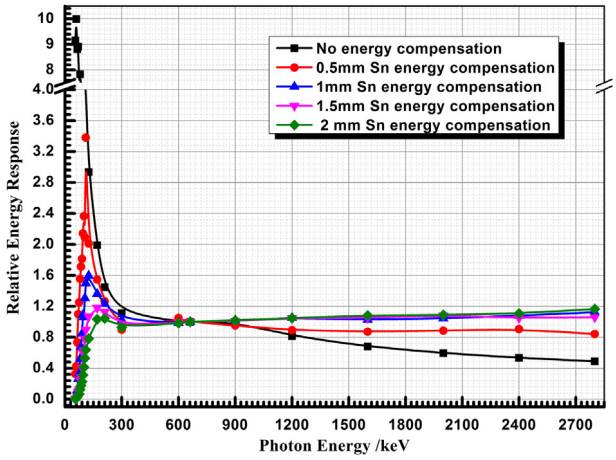

Fig. 8. Relative energy response curves of small-volume GM counters.

was performed to prove the necessity of 3G. Buildings shade the signal; thus, the RF transmission will fail.

3. Experimental results and discussions

Generally, GM counters are used as air absorbed dose rate detector. The energy response is the ratio of the count of GM counters to the air absorbed dose rate, and the number of electron entered into sensitive volume is approximately equal to the count of GM counters. Therefore, the air absorbed dose rate and the number of electron entered into sensitive volume were recorded by MCNP5. The calculated relative energy dependence (normalized at 662 keV) of the large-volume GM counter are shown in Fig. 7.

As seen in Fig. 7, the trends of the four response curves are different; the order of the compensation ability is Pb > Sn > Cu > Al, which is also the order of the gamma attenuation ability. The front of the Al-compensated curve is too high to accomplish the purpose of the compensation. Although Cu has a better effect than Al, the energy response of the GM counter for the 100–200 keV photons is still relatively high. Therefore, Al and Cu are not appropriate for energy compensation, whereas Pb and Sn showed very excellent effects. Pb

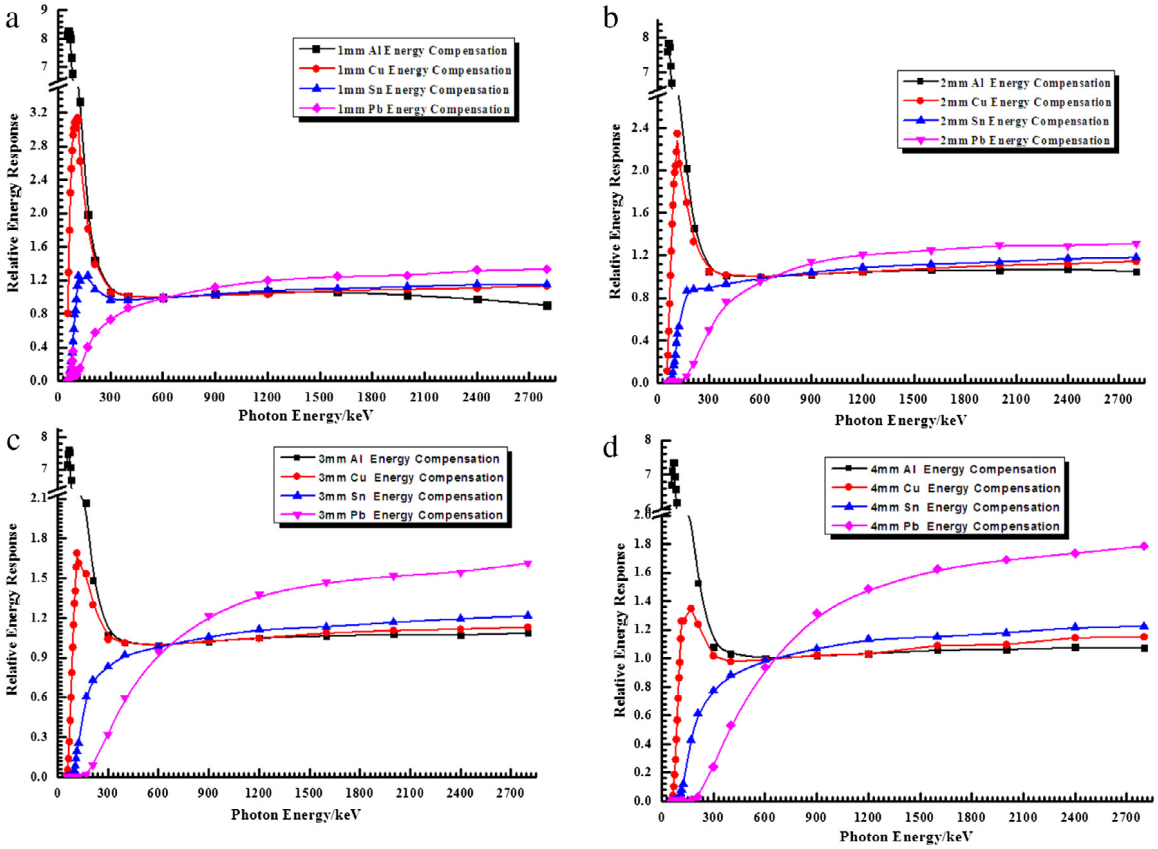

Fig. 7. Relative energy response curves of large-volume GM counters.

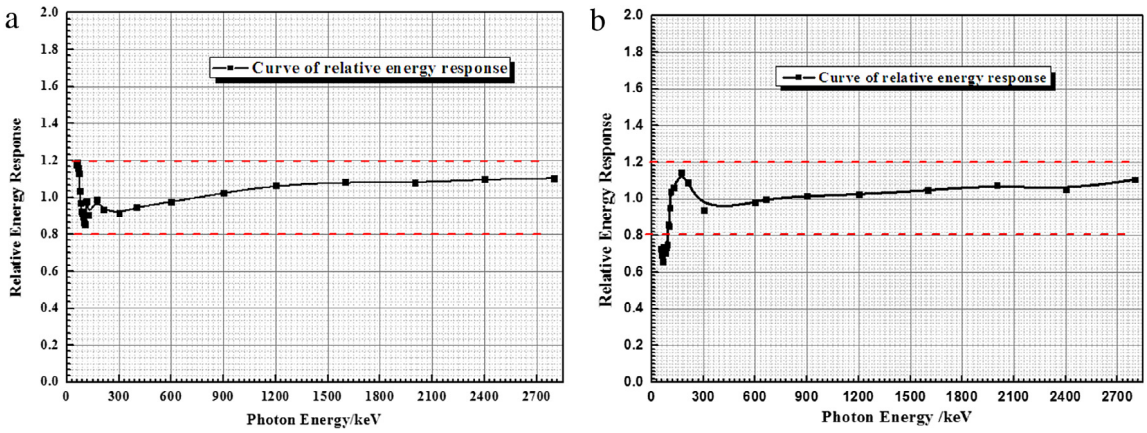

Fig. 9. Relative energy response curves of GM counters after compensation.

has a very strong absorption of 90 keV gamma rays; thus, the energy compensation is uneven. This compensation ranges from 55 to 100 keV. Fig. 7(a) shows an obvious single peak in the curve. This non-uniformity complicates the process of energy compensation; thus, the amount of Pb is also inappropriate. Put simply, based on these calculations, the best single wrapper was considered to be 2 mm of Sn of the cases simulated.

Given the above-mentioned conclusion, we can conclude that only Sn can satisfy the energy compensation needs. The effects of four different thicknesses Sn were simulated, and calculation processes of small-volume and large-volume GM counters were similar.

Given the increasing thickness, the compensation effect of small-volume GM counter in (Fig. 8) gradually improved. The end of the curve (300–2800 keV) is quite flat. The optimal layer thickness of Sn is 2 mm. The compensation effect of the 2 mm-thin compensation can meet the demands of energy response.

Figs. 7 and 8 clearly show that the response to low-energy gamma is insufficient. To resolve this problem, GM counters were usually not completely covered by the metal layer. Some of the GM counters should be exposed to compensate for the low-energy response. Based on Eq. (1), we optimized the proportion of the exposed portion as:

$$R = p \times r_0 + (1 - p) \times r_n, \tag{1}$$

where R is the relative energy response of the completed compensation; p is the proportion of the exposed portion; r_0 is the relative energy response of the GM counter without a metal layer; r_n is the relative energy response with the metal layer.

The ideal result after the completion of energy compensation is that the relative energy response is 1 for each energy level. That is, the photon energy does not have a significant effect on the measurement accuracy. In the optimized result, the proportion of the exposed part of the large-volume GM counter is 20%, whereas that of the smaller counter is 15%. GM counters with the slit metal layer were also simulated by MCNP 5; the results are shown in Fig. 9. The slit was located in the middle of the GM counter. With the exception of the slit, other aspects were similar to the GM counters that were perfectly wrapped. The simulation results of the large-volume GM tube are shown in Fig. 9(a); results of the small-volume GM tube are shown in Fig. 9(b).

After the compensation, the relative energy response of the GM counter is almost equal to 1 at 90–2800 keV (Fig. 9). Compared with the results in Fig. 8, the end of the response curve did not change, but significant differences were observed before and after split in the range of 90–300 keV. The wall of the large-volume GM counter is slightly thicker than that of the small-volume GM counter. The sensitive volume of the large-volume GM counter is higher than that of the small-volume GM counter. Therefore, the slit compensation had better effects on the large-volume GM counter than the small-volume GM counter. The results showed that the relative energy response of the new detector is less than 20% in the range of 90–2800 keV, and it is possible to place with two or more metals for energy compensation in the future if higher accuracy is needed.

The time-to-count technology converted the number of traditional measurements to the average time of the interval time between two pulses [20]. The reciprocal of the time interval is related to environmental dose rate. Given a low dose rate, the interval time between two pulses per unit time is both long and variable; thus, the smoothing time is extended to 6 s to reduce the influence of randomness. The results from the standard dose field are shown in Fig. 10. The calibration result measured by the large-volume GM counter is shown in Fig. 10(a), whereas those measured by the small-volume GM counter are shown in Fig. 10(b).

The calibration curves of the standard dose field differed from those of the traditional measurement (Fig. 10). The front slope of the calibration curves is relatively large because the pulse number is lower, and the statistical fluctuation affected the linear curve. Based on the average time interval, the microprocessor automatically switched GM tubes. Because the MCU needed time to execute the program, the minimum resolution time is 1 μs. When changing from the large-volume GM counter to the small volume GM tube, the average time interval was 5 μs. In order to ensure the accuracy of the data, the average time interval must be no too long. When switching from the small-volume GM counter to the large volume GM tube, the average time interval was 10,000 μs. A pairwise function showed the relationship between the reciprocal of the time interval and the radiation dose rate, which is composed of a quadratic function and a linear function. When the pulse number is lower, the relation between the reciprocal of the time interval and the radiation dose rate is a quadratic function.

In an outdoor experiment, the environment dose rate was measured for every 1 m. GPS could offer the location information in the data terminal. We tested 121 points to produce the dose distribution map. As shown in Fig. 11(a), two sources could be clearly found by the color filled contour map.

The data in Fig. 11(b) is concentrated in an area, with a slightly decreasing trend. Given that the half-life of I-131 is approximately 8 days, the source activity gradually declined over the 11 h period. The measurement data was more consistent. The measurement error was usually less than 10%. These experiments proved that the portable dose rate detector can be used for unattended tasks.

4. Conclusions

The double GM counter, the portable dose rate detector described was developed for daily radiation monitoring and nuclear accident emergency. It has a wide dynamic range and is straight forward to suitable for varieties of application. This instrument is a new development of traditional GM counter detectors. By adding the GPS, 3G, and

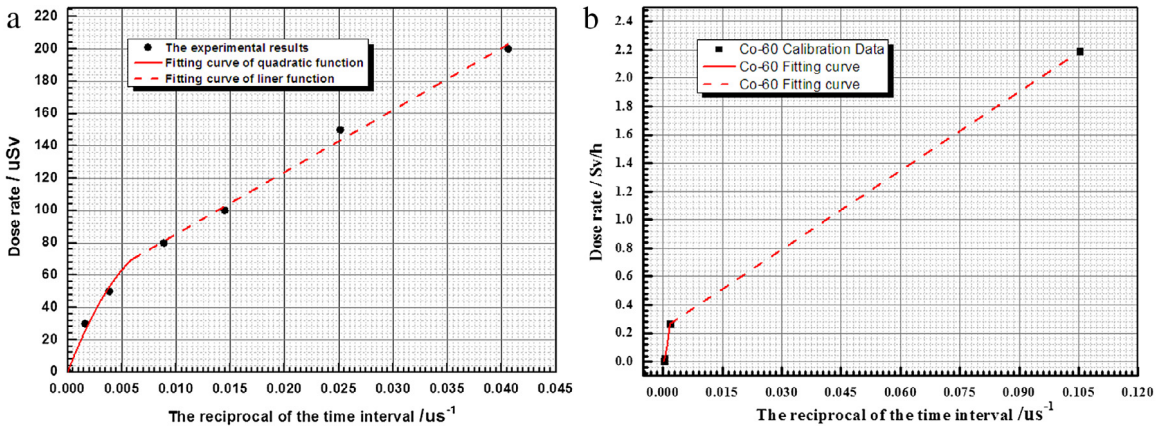

Fig. 10. Calibration curve of large-volume and small-volume GM counters.

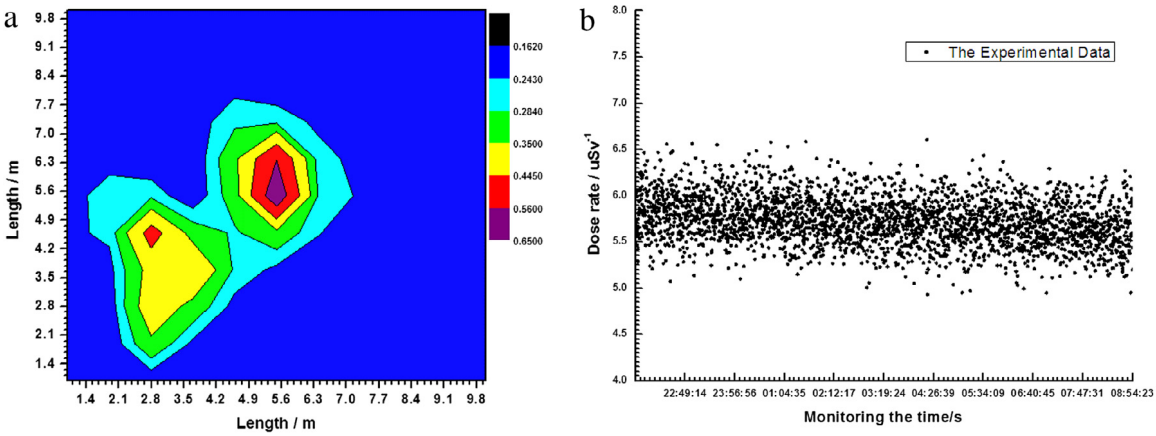

Fig. 11. Results of the experiment of the actual environment.

RF functions, the application scope was broadened. The calibration of the standard dose rate and testing experiments demonstrates that the detector can be applied commendably in practice.

Acknowledgments

The present work was supported by Project supported by the National Natural Science Foundation of China (Grant No. 11675078); The National Defense Basic Scientific Research Project (Grant No. B2520133007); The Priority Academic Program Development of Jiangsu Higher Education Institutions and the Project supported by the Fundamental Research Funds for the Central Universities (Grant No. NJ20160034).

References

[1] K. Saito, N. Petoussi-Henss, M. Zankl, Calculation of the effective dose and its variation from environmental gamma ray sources, Health Phys. 74 (1998) 698–706.
[2] A. Osovizky, D. Ginzburg, A. Manor, R. Seif, M. Ghelman, I. Cohen-Zada, M. Ellenbogen, V. Bronfenmakher, V. Pushkarsky, E. Gonen, SENTIRAD—An innovative personal radiation detector based on a scintillation detector and a silicon photomultiplier, Nucl. Instrum. Methods Phys. Res. Sect. A 652 (2011) 41–44.
[3] M. Munir, N. Ahmad, S. Sohail, R.A. Naveed, M.Q. Rafiq, M. Khalid, Design and development of a portable gamma radiation monitor, Rev. Sci. Instrum. 80 (2009) 073101.
[4] H. Sato, A. Yamaguchi, O. Maida, T. Ito, Survey meter combining CVD diamond and silicon detectors for wide range of dose rates and high accumulated doses, Radiat. Meas. 47 (2012) 266–271.
[5] I. Meric, G.A. Johansen, M.B. Holstad, A.F. Calderon, R.P. Gardner, Enhancement of the intrinsic gamma-ray stopping efficiency of Geiger–Müller counters, Nucl. Instrum. Methods Phys. Res. Sect. A 696 (2012) 46–54.
[6] G. Knoll, G. Knoll, Radiation Detection and Measurement, third ed, 2000.
[7] T. Watanabe, A computational analysis of intrinsic detection efficiencies of Geiger–Mueller tubes for photons, Nucl. Instrum. Methods Phys. Res. Sect. A 438 (1999) 439–446.
[8] M. Yousaf, T. Akyurek, S. Usman, A comparison of traditional and hybrid radiation detector dead-time models and detector behavior, Prog. Nucl. Energy 83 (2015) 177–185.
[9] E.J. Diianni, H.J. Cooley, M. Fujita, C.V. Noback, Radiation Measuring Apparatus, US, 1986.
[10] K. Parameshwaran, Design and Implementation of Biomesensi Software Platform, California State University, Long Beach, 2015.
[11] Developers, Architects, The Definitive Guide to the ARM Cortex-M3, 2007.
[12] J.H. Davies, A basic introduction to Cadence OrCAD PCB Designer Version 16.3, 2011.
[13] K. Stanković, P. Osmokrović, The model for calculating the type a measurement uncertainty of GM counters from the aspect of device miniaturization, IEEE Trans. Nucl. Sci. 61 (2014) 1316–1325.
[14] D.H. Wilkinson, The Geiger discharge revisited Part I. The charge generated, Nucl. Instrum. Methods Phys. Res. Sect. A 321 (1992) 195–210.
[15] D. Wilkinson, The Geiger discharge revisited Part II. Propagation, Nucl. Instrum. Methods Phys. Res. Sect. A 383 (1996) 516–522.
[16] D. Wilkinson, The Geiger discharge revisited Part III. Convergence, Nucl. Instrum. Methods Phys. Res. Sect. A 383 (1996) 523–527.
[17] D. Wilkinson, The Geiger discharge revisited Part IV. The fast component, Nucl. Instrum. Methods Phys. Res. Sect. A 435 (1999) 446–455.
[18] D. Barclay, Improved response of Geiger muller detectors, IEEE Trans. Nucl. Sci. 33 (1986) 613–616.
[19] H. Zhu, S. Kane, S. Croft, R. Venkataraman, Optimization of the Canberra UltraRadiac GM tube wrapping, IEEE Trans. Appl. Supercond. 2 (2006) 923–925.
[20] O. Vagle, Ø. Olsen, G. Johansen, A simple and efficient active quenching circuit for Geiger–Müller counters, Nucl. Instrum. Methods Phys. Res. Sect. A 580 (2007) 358–361.